Superhydrophobic Films

Tunable, Superhydrophobically Stable Polymeric Surfaces by Electrospinning**

*Kazim Acatay, Eren Simsek, Cleva Ow-Yang, and Yusuf Z. Menceloglu**

The high water repellence of superhydrophobic surfaces is attributed to the limited contact area between the solid and water which is manifested by a high static water contact angle (WCA) and a low sliding angle. The solid–liquid interfacial energy can be minimized by engineering not only the chemistry but also the topography of the solid surface.[1,2] For example, epicuticular wax on the lotus leaf is an intrinsically hydrophobic material.[3] However, when nano-sized crystals of wax cover a micron-level rough surface, as is the case on the lotus leaf, the WCA is further enhanced to 160°, which is defined as superhydrophobic.[4–8] In this case, the water droplet forms a three-dimensional, discontinuous, triphasic (water–air–solid) contact line[9] that is relatively longer and less stable than such a line on a macroscopically smooth surface. Moreover, a nonhydrophobic material can also be rendered hydrophobic with a WCA well above 150° by chemical modification, for example, through the incorporation of fluorine or silicone, as well as by increasing the roughness.[9–14] Such an extreme water repellence is highly attractive for novel industrial and practical applications: continuously clean buildings, windows, and outdoor decorations, stain-resistant fabrics, antifouling marine structures, and oxidation-resistant surfaces.[2,8,10] Currently, the production of superhydrophobic surfaces is based on time-consuming, expensive, and/or nonversatile processes, such as controlled crystallization, lithography, etching, and templating.[9–13,15]

To mimic the topography of the lotus leaf and to achieve a high WCA, we fabricated a polymeric film surface with a high degree of roughness through a simple and practical electrospinning process.[16] Electrospun films consist of a continuous, nonwoven web of fibers (with diameters in the order of 1–1000 nm) and, depending on processing conditions, with polymer droplets either as isolated spheres ($>1\,\mu m$ in diameter) or strung along a fiber.[17–22] The electrospun film is produced by applying an electrical bias from the tip of a polymer solution-filled syringe to a grounded collection plate. Along the trajectory of the extruded polymer fiber, most of the solvent evaporates, such that a mat of randomly aligned fibers collects and form a thin film. In addition to surface roughness, the film properties were optimized by chemical modification, such as the addition of fluorine to enhance and stabilize WCA values and the incorporation of crosslinking for solvent resistance. Our ability to engineer both the physical and chemical properties of the electrospun films enables flexibility in tuning the degree of hydrophobicity.

A thermoset polymer was synthesized by first reacting acrylonitrile (AN) and α,α-dimethyl *meta*-isopropenylbenzyl isocyanate (TMI) in *N*,*N*-dimethylformamide (DMF), and then mixing the resultant poly(AN-co-TMI) with a perfluorinated linear diol (fluorolink-D) and tin(II) ethyl hexanoate (T2EH) in DMF. The solution was mixed and immediately electrospun onto an aluminum foil substrate covering the electrically grounded screen. The processing parameters used throughout this study were fixed for the 30-min electrospinning periods: tip-to-ground distance 10 cm, flow rate of the polymeric mixture 12.5 $\mu L\,min^{-1}$, spinning voltage 16 kV. The remaining mixture was subsequently cast onto microscope slides for wetting comparison. The electrospun samples and the corresponding cast films were subsequently annealed at 70 °C for at least 8 h, which enabled the reorientation of the perfluorinated groups to the solid–air interface.[22] A comparison of the measured static WCA between an electrospun film and a cast version of the same composition reveals an enhancement of up to 60° (Figure 1a and b).

One parameter that allowed the topography of the electrospun film to be tuned was the viscosity, which we investigated by mixing poly(AN-co-TMI) with fluorolink-D (50 wt%) in various quantities of DMF to create a range of viscosities (31–350 mPa s). As the viscosity increased, the morphology of the micro-textured films changed from one containing predominantly beads to another of only fibers, as

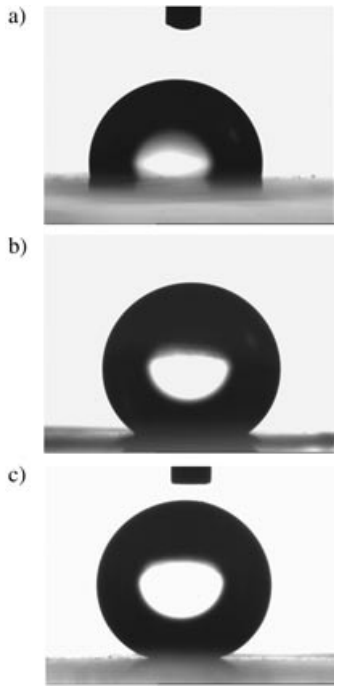

Figure 1. Photographs taken during WCA measurements: a) cast film of 31 mPa s mixture (WCA = 96°), b) electrospun film of 31 mPa s mixture (WCA = 156°), and c) electrospun low-molecular-weight (LMW) copolymer (WCA ≈ 167°).

[*] Dr. K. Acatay, E. Simsek, Dr. C. Ow-Yang, Prof. Y. Z. Menceloglu
Materials Science and Engineering Program
Faculty of Engineering and Natural Sciences
Sabanci University
Orhanli 34956 Tuzla-Istanbul (Turkey)
Fax: (+90) 216-483-9550
E-mail: yusufm@sabanciuniv.edu

[**] We thank Cytec and Ausimont for their kind donations of TMI and fluorolink-D, respectively.

  DOI: 10.1002/ange.200461092

revealed by scanning electron microscope (SEM) imaging (Figure 2a,b,c). A surface consisting of mostly 2–3-μm diameter beads can be rougher than a surface covered with 200–400-nm thick fibers. Moreover, the bead-rich topography

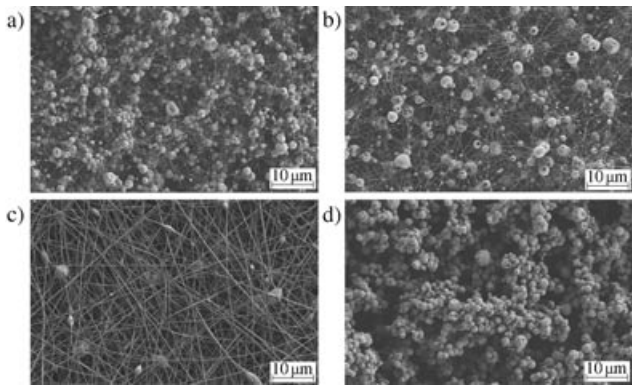

Figure 2. Scanning electron microscope images of electrospun films of copolymers with viscosities: a) 31 mPa s, b) 102 mPa s, and c) 348 mPa s (HMW copolymer), and d) 51 mPa s (LMW copolymer). The measurements were carried out at 1 keV and 5000× magnification.

increases the discontinuities in the triphasic contact line[11] much more than does the fiber-rich surface. The measured static WCA of the films ranged from 156° (for a solution viscosity of 31 mPa s) to 148° (350 mPa s), with a maximum standard deviation of ±2°. In contrast, cast films of corresponding compositions yielded WCAs in the range 96–99°.

Because the tilt angle of a superhydrophobic surface indicates the water–solid interface energy that immobilizes a water droplet, the self-cleaning ability of a surface can effectively be characterized by the threshold sliding angle. We determined the sliding angle of a water drop on an electrospun sample by placing a 10–mg drop of water on the textured film surface, which was then inclined at increasing angles until the drop started to roll. As the fiber content increased on our micro-textured surfaces, we observed a concurrent increase in sliding angle: Figure 2a, tilt angle = 20.7 ± 7.5°; Figure 2b, tilt angle = 52.6 ± 5.6°; Figure 2c, no rolling at 90° tilt.

The viscosity study suggested that the WCA on our micro-textured surfaces increased as the bead ratio increased, implying that a surface morphology containing solely beads may generate even larger WCAs. However, the use of a polymer solution with a viscosity lower than 31 mPa s for electrospinning produced surfaces with low roughness, because the non-evaporated solution also reached the grounded plate. In the electrospinning of low-molecular-weight polymer solutions, extensive droplet formation was observed[23] which was attributed to Rayleigh instability in the fluid flow. In fact, more beads form as the molecular weight of the polymer decreases. Thus as expected, we observed a direct relationship between the molecular weight of poly(AN-co-TMI) and the WCA on the electrospun film. A poly(AN-co-TMI) substance of low molecular weight was synthesized by changing the polymerization reaction solvent from *N*,*N*-dimethylformamide (DMF) to tetrahydrofuran (THF), while using the same reactant ratio, temperature, and time. When the viscosity average molecular weight of the polymers was measured, we found that the copolymer synthesized in DMF has a higher molecular weight (~20000 g mol^{-1}, the HMW copolymer), whereas the copolymer synthesized in THF has a lower molecular weight (~4000 g mol^{-1}, the LMW copolymer). When the LMW copolymer was mixed with fluorolink-D and electrospun (51 mPa s), the electrospun film consisted of only clustered polymeric beads ranging from 1 to 3 μm in diameter (Figure 2d). In contrast, when the HMW copolymer with a similar viscosity was electrospun under the same processing conditions, the result was a fibrous morphology also containing beads (Figure 2a). The static WCA of 166.7 ± 2.2° measured on the electrospun LMW copolymer (Figure 1c), was the maximum average WCA that we have obtained for the electrospun films. Also, the relatively low tilt angle of 4.3 ± 0.8° indicated that this film is more suitable for self-cleaning applications than the fiber-containing, electrospun films. Evidently, the presence of fibers decreases the variation in roughness amplitude, so that a film morphology of predominantly beads enhances water immobilization owing to a long and discontinuous interface at the bottom of the droplet. In contrast, a mat of fibers creates a nano-textured surface that is relatively smooth at the micron level.

Recently, there has been much discussion in the literature about the stability of the superhydrophobic state of micro-textured surfaces, which effectively determines the potential for the self-cleaning behavior of these surfaces.[1,7] Two different equilibrium states defined in the literature for rough superhydrophobic surfaces are the Cassie[24] and Wenzel[25] states. The Wenzel state exhibits a high WCA owing to an increase in surface area, whereas the Cassie state describes a high WCA owing to trapped air pockets in the rough surface. The Cassie regime offers a lower hysteresis between advancing and receding WCAs, because the water droplet is mostly in contact with the trapped air, and the hydrophobic surface has a lower sliding (roll-off) angle. On the other hand, because the Wenzel regime is a consequence of a larger water–solid interface energy pinning that fixes the droplet to the film surface, the hysteresis is larger, and the droplet cannot slide as easily.

However, the type of superhydrophobic state is not always clearly either Cassie or Wenzel in nature, and can be misleadingly designated as a metastable Cassie state.[7] To understand how such a metastable Cassie state can simultaneously exist with a Wenzel state, consider a water drop sitting on a surface of the metastable Cassie-type. If this drop is uniaxially loaded above a material-specific threshold level, the trapped air in the pockets is irreversibly pushed out and replaced with water, and the increase in surface contact area is accompanied by a sudden decrease in the postpressing WCA values. Thus, the water drop is immobilized, the Cassie state is irreversibly transformed into the Wenzel state, and the self-cleaning ability of the surface is lost. Moreover, owing to the increased adhesion to both pressing plates, upon release of the load, the drop can split into two hemispheres, with one half adhering to the top plate, and the other half to the bottom plate.

To determine the hydrophobic state of our textured films, water droplets were placed between two plates covered with HMW copolymer electrospun films (Figure 2a,b), and uniaxially loaded (Figure 3). We were able to load the water

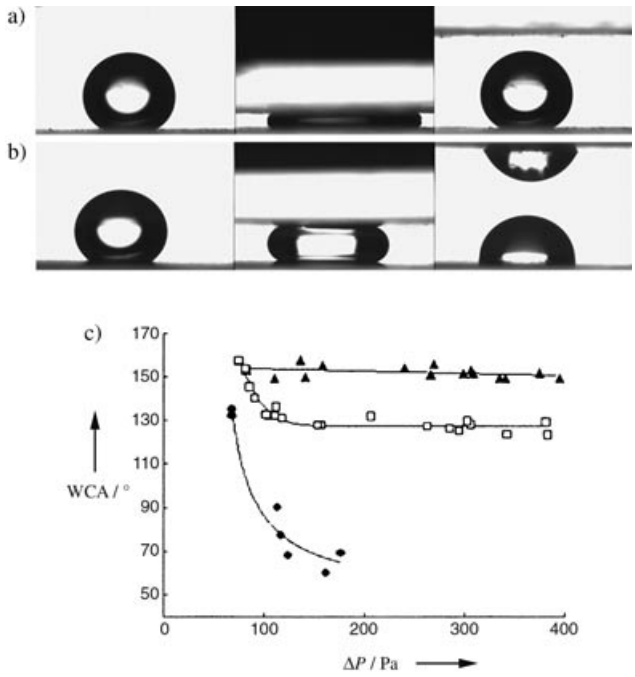

Figure 3. Water droplet pressing between two identical surfaces of: a) 31 mPa s electrospun at Figure 2a. b) 348 mPa s electrospun at Figure 2c. Photos were taken before, during, and after pressing of the droplet. c) Plot showing the variation in measured postpressing WCA of droplets versus applied pressure (ΔP) for fluorinated HMW copolymer surfaces (▲ 31 mPa s, □ 102 mPa s, ● 348 mPa s.

droplets up to 350–400 Pa (calculated by using the Laplace equation[7]) and to measure the static postpressing WCAs (Figure 3c). As the fiber ratio increases, the postpressing WCA of the textured surfaces decreases, following trends observed in the static WCA and sliding angle analyses. The static WCA of the electrospun film at Figure 2a does not change even at 400 Pa (Figure 3a), which is consistent with a very stable Cassie state of superhydrophobic behavior and the two-level roughness condition stipulated by Lafuma and Quéré.[7] However, for films electrospun from the solution with a viscosity of 102 mPa s (Figure 2b), the postpressing WCAs stabilized at 125° at roughly 400 Pa (≈30° decrease in WCA). Figure 3b shows that the water droplet had split into two hemispheres under a load of ≈80 Pa for the film described in Figure 2c. Although this experiment was not performed on the sample with the bead-only morphology owing to the insufficient mechanical integrity of the film, we can still conclude from the trend in our observations that as the fiber ratio of the fluorinated samples increases, the textured surface begins to exhibit an unstable, Wenzel-type superhydrophobicity.

To achieve a stable (Cassie) superhydrophobic state, a material must have a surface topography of at least bilevel roughness in addition to being chemically hydrophobic. In fact, there are actually three levels of roughness on our samples with the higher WCAs. To see this third level, consider the uniform height of lithographically patterned, superhydrophobic surfaces. Our samples showed an even broader distribution in roughness amplitude, creating yet another macroscopic level of roughness. Because this gave rise to a much longer triphasic contact line with more discontinuities, the water–solid interface energy was consequently lowered, and the water drop moved more readily on the stable superhydrophobic surface, consistent with the Cassie model.[12] We speculate that the irregular, micron-level fluctuations in amplitude enabled our films to achieve a stable superhydrophobic state with a WCA exceeding that of the lotus leaf. Manipulation of the water–solid interface energy enabled us to produce extremely water-repellent, potentially self-cleaning, stable coatings by a simple electrospinning process.

Experimental Section

The acrylonitrile (AN, Merck) was used after purification by double distillation over CaH_2 under nitrogen. DMF (Aldrich), THF (Aldrich), AIBN (Fluka), TMI (Cytec), and fluorolink-D (Ausimont) were all used as received.

The viscosity average molecular weight of poly(AN-co-TMI) (AN:TMI ≈ 10:1 was measured on a Cannon Ubbelohde Viscometer (Size 1B). During calculations, the constants of polyacrylonitrile (PAN) in DMF at 25 °C ($K = 39.2 \times 10^{-5}$ and $a = 0.75$) were used. Viscosities of the polymer solutions were measured on a DV-III Rheometer (Brookfield) coupled with a Wells-Brookfield Cone/Plate. SEM imaging of the electrospun films was performed on a LEO Supra VP35 FE-SEM, after sputter deposition of a thin conductive gold coating onto the films. The CAs were measured on a Krüss GmbH DSA 10 Mk 2 goniometer with DSA 1.8 software. At least ten droplets of 5 mg freshly distilled ultrapure water were averaged. For sliding-angle measurements, at least ten 10-mg water droplets were placed onto the films, and slowly inclined by a simple system.

Received: June 26, 2004

Keywords: electrospinning · hydrophobic effects · nanostructures · polymers · surface chemistry

[1] D. Quere, A. Lafuma, J. Bico, *Nanotechnology* **2003**, *14*, 1109.
[2] A. Nakajima, K. Hashimoto, T. Watanabe, *Monatsh. Chem.* **2001**, *132*, 31.
[3] S. Herminghaus, *Europhys. Lett.* **2000**, *52*, 165.
[4] R. Blossey, *Nat. Mater.* **2003**, *2*, 301.
[5] W. Barthlott, C. Neinhuis, *Planta* **1997**, *202*, 1.
[6] C. Neinhuis, W. Barthlott, *Ann. Bot.* **1997**, *79*, 667.
[7] A. Lafuma, D. Quéré, *Nat. Mater.* **2003**, *2*, 457.
[8] P. Gould, *Mater. Today* **2003**, *6*, 44.
[9] D. Oner, T. J. McCarthy, *Langmuir* **2000**, *16*, 7777.
[10] H. Y. Erbil, A. L. Demirel, Y. Avcý, O. Mert, *Science* **2003**, *299*, 1377.
[11] W. Chen, A. Y. Fadeev, M. C. Hsieh, D. Öner, J. Youngblood, T. J. McCarthy, *Langmuir* **1999**, *15*, 3395.
[12] M. Miwa, A. Nakajima, A. Fujishima, K. Hashimoto, T. Watanabe, *Langmuir* **2000**, *16*, 5754.
[13] S. R. Coulson, I. Woodward, J. P. S. Badyal, S. A. Brewer, C. Willis, *J. Phys. Chem. B* **2000**, *104*, 8836.
[14] L. Feng, S. Li, H. Li, L. Zhang, J. Zhai, Y. Song, B. Liu, L. Jiang, D. Zhu, *Adv. Mater.* **2002**, *14*, 1857.

[15] a) L. Feng, S. Li, H. Li, L. Zhang, J. Zhai, Y. Song, B. Liu, L. Jiang, D. Zhu, *Angew. Chem.* **2002**, *114*, 1269; *Angew. Chem. Int. Ed.* **2002**, *41*, 1221; b) Y. Zhao, J. Zhai, L. Jiang, *Angew. Chem.* **2004**, *116*, 4438; *Angew. Chem. Int. Ed.* **2004**, *43*, 4338.
[16] K. Acatay, Y. Z. Menceloglu, M. A. Gulgun, PCT/TR03/0067, **2003**.
[17] Z.-M. Huang, Y.-Z. Zhang, M. Kotaki, S. Ramakrishna, *Compos. Sci. Technol.* **2003**, *63*, 2223.
[18] J. Doshi, D. H. Reneker, *J. Electrost.* **1995**, *35*, 151.
[19] M. M. Demir, M. A. Gulgun, Y. Z. Menceloglu, B. Erman, S. S. Abramchuk, E. E. Makhaeva, A. R. Khokhlov, V. G. Matveeva, M. G. Sulman, *Macromolecules* **2004**, *37*, 1787.
[20] Y. M. Shin, M. M. Hohman, M. P. Brenner, G. C. Rutledge, *Polymer* **2001**, *42*, 9955.
[21] H. Fong, I. Chun, D. H. Reneker, *Polymer* **1999**, *40*, 4585.
[22] J. M. Deitzel, W. Kosik, S. H. McKnight, N. C. BeckTan, J. M. DeSimone, S. Crette, *Polymer* **2002**, *43*, 1025.
[23] A. Koski, K. Yim, S. Shivkumar, *Mater. Lett.* **2004**, *58*, 493.
[24] A. B. D. Cassie, S. Baxter, *Trans. Faraday Soc.* **1944**, *40*, 546.
[25] R. N. Wenzel, *Ind. Eng. Chem.* **1936**, *28*, 988.

